International Institute for
Applied Systems Analysis
Schlossplatz 1
A-2361 Laxenburg, Austria

Tel: +43 2236 807 342
Fax: +43 2236 71313
E-mail: publications@iiasa.ac.at
Web: www.iiasa.ac.at

Interim Report **IR-13-069**

Population-level consequences of heterospecific density-dependent movements in predator-prey systems

Henrik Sjödin
Åke Brännström (brnstrom@iiasa.ac.at)
Mårten Söderquist
Göran Englund

Approved by

Ulf Dieckmann
Director, Evolution and Ecology Program

June 2015

Population-level consequences of heterospecific density-dependent movements in predator-prey systems

Henrik Sjödin[a,*], Åke Brännström[b,c], Mårten Söderquist[a], Göran Englund[a,**]

[a] *Department of Ecology and Environmental Science, Umeå University, 90187 Umeå, Sweden*
[b] *Department of Mathematics and Mathematical Statistics, Umeå University, 90187 Umeå, Sweden*
[c] *Evolution and Ecology Program, International Institute for Applied Systems Analysis, 2361 Laxenburg, Austria*

Abstract

In this paper we elucidate how small-scale movements, such as those associated with searching for food and avoiding predators, affect the stability of predator-prey dynamics. We investigate an individual-based Lotka-Volterra model with density dependent movement, in which the predator and prey populations live in a very large number of coupled patches. The rates at which individuals leave patches depend on the local densities of heterospecifics, giving rise to one reaction norm for each of the two species. Movement rates are assumed to be much faster than demographics rates. A spatial structure of predators and prey emerges which affects the global population dynamics. We derive a criterion which reveals how demographic stability depends on the relationships between the per capita covariance and densities of predators and prey. Specifically, we establish that a positive relationship with prey density and a negative relationship with predator density tend to be stabilizing. On a more mechanistic level we show how these relationships are linked to the movement reaction norms of predators and prey. Numerical results show that these findings hold both for local and global movements, i.e., both when migration is biased towards neighboring patches and when all patches are reached with equal probability.

1. Introduction

Small scale movements, such as those associated with searching for food and avoiding predators, affect encounter rates between predators and prey and thus their large scale population dynamics (Krivan 1997; Abrams 2007; Flaxman et al. 2011). It is therefore essential to clarify the links between such movements, the spatial patterns that they create, and the intensity of the associated trophic interactions in order to properly understand food web dynamics (Dieckmann et al. 2001; Murdoch et al. 2003). A range of modeling approaches have been used to study the relationship between small scale movements and predator-prey dynamics, reflecting the wide variety of movements that different organisms perform. Crucial aspects that motivate different model assumptions are the spatial and temporal scales of movements and the degree to which organisms base their movement decisions on information about the abundance of competitors, predators, and resources.

Small-scale movements, such as foraging and avoiding predators, typically occur on a much faster time scale than birth and death processes. If such movements are random, they lead to perfect mixing and thus do not alter the outcomes predicted when using non-spatial predator-prey models. However, non-random spatial distributions that affect interaction rates can be produced if movements are reactive, i.e., if movement rates depend on local densities of competitors and predators or habitat quality (Bell et al. 2009; Flaxman et al. 2011). This study focuses on heterospecific density-dependent movements of predators and prey. Prey typically avoid areas with high predator densities, whereas predators tend to prefer areas with high prey densities. These conflicting goals give rise to a spatial game that has been termed a space race (Sih 2005). Studies of space race games and other habitat selection games, have derived evolutionary stable distributions and investigated whether or not density-dependent movements lead to such distributions (Iwasa 1982; Cressman et al. 2004; Schreiber and Vejdani 2006; Abrams 2007; Krivan et al. 2008).

Studies of the effects of space races on large scale population dynamics have focused on the Lotka-Volterra predator-prey model and the Nicholson-Bailey host-parasitoid model. The effects on stability are variable, although stabilizing effects seem to predominate (van Baalen and Sabelis 1993; Krivan 1997, 1998; van Baalen and Sabelis 1999; Cressman et al. 2004; Mchich et al. 2007). An interesting exception is the tri-trophic model of Abrams (2007), which differs from other models in that it assumes that the timescales of the studied movements are similar to those for the rates of birth and death. These studies use stringent simplifying assumptions that make it possible to formulate analytically tractable models. For example, it is typically assumed that habitats have a limited number of patches (usually two) and that organisms are omniscient and obey deterministic movement rules without errors. To evaluate the generality of findings obtained using such models it is useful to compare them to results obtained using models that are based on more realistic assumptions. For example, populations living in large habitats typically have limited information about patch qualities and may therefore use movement rules that do not necessarily produce evolutionarily stable distributions. Moreover, it can be argued that the movements that occur according to such rules are best described as stochastic processes because they are based on uncertain information and may involve interactions with small numbers of individuals. Although such scenarios have been studied using individual-

*henrik.sjodin@emg.umu.se
**goran.englund@emg.umu.se

Preprint submitted to Elsevier

based spatially explicit simulation models (e.g., Flaxman et al. 2011), it is important to develop analytical models that can be used to enhance our mechanistic understanding of the effects of predator-prey space races on spatial distributions and population dynamics.

In this study we analyze a stochastic space race model where predators and prey use density-dependent movement rules. Our analysis yields analytical approximations that describe the statistical moments of the spatial distributions as functions of the global mean densities of predators and prey. We then investigate how the resulting covariance between predator and prey densities affects the stability of the Lotka-Volterra predator-prey model. We find that the stability is determined by the relationships between the per capita covariance and the global mean densities. Specifically, the dynamics are stabilized by a positive relationship with prey density and negative relationship with predator density. On a more mechanistic level we show how these relationships are linked to the movement reaction norms of predators and prey.

2. Model

2.1. Overview

Assume that a space is divided into a very large number of compartments, henceforth referred to as patches, and that in this space individuals of a predatory species p and a prey species n interact locally in patches between which they can move. In each and every patch, at any given time, there are an integer number of prey individuals X_n and predator individuals X_p, and the corresponding global spatial expectations are $\langle X_\mathrm{n}\rangle$ and $\langle X_\mathrm{p}\rangle$, respectively. The probability per unit time $\mathrm{d}t$ that the number of individuals of each species will change by one individual is governed by transition processes T, i.e., birth, death and movement. These processes produce spatial patterns that can be described in terms of the distribution of patch frequencies $D(x_\mathrm{n}, x_\mathrm{p}, t)$. Furthermore, assume that the patches are so small that there is perfect mixing of individuals within patches and that the processes governing movements between patches are much faster (taking place on the time-scale $\mathrm{d}\tau$) than the processes governing vital events (birth and death, which occur on the time-scale $\mathrm{d}t$). Given these assumptions, the interactions between predators and prey can be described using a stochastic individual-based Lotka-Volterra model, using stochastic movement rules to model migration between patches.

As a starting point, we assume that movements are global, i.e., individuals move from patches to a dispersal pool where they instantly mix and return to other randomly chosen patches in equal numbers (figure 1). The probability of leaving a patch during a single small time step depends on the number of predators or prey in that patch, whereas the number of individuals immigrating to a given patch is independent of local abundances − this reflects the assumption that each individual is aware of their current environment but does not have information on their destination environment. With global movements, the rate of immigration to any given patch is equal to the average rate of emigration from all patches. In most natural systems, movements are local rather than global, i.e. most movements occur between neighboring patches. In section Robustness, we present numerical evidence that our results derived for global movements also holds for local movements.

A global predator-prey model is obtained by averaging over all local processes. This global model is a deterministic approximation that incorporates both movements in space and ecological dynamics.

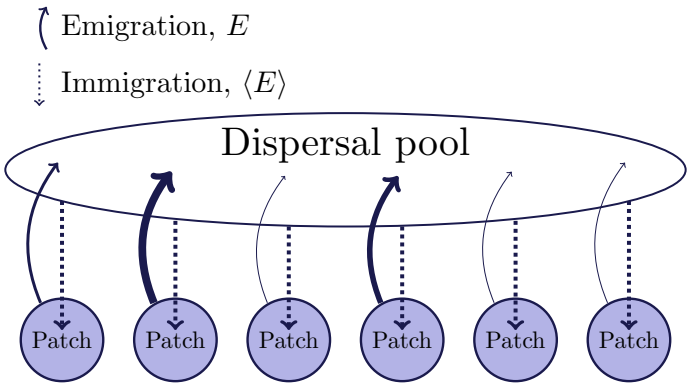

Figure 1: A graphical representation of a global movement process, here exemplified using a linear array of six patches. The process can be thought of as that emigrants (curved arrows) move from patches to a dispersal pool where they instantly mix and return to every patch in equal numbers. The rates of emigration from each patch depend on its numbers of predators and prey, whereas the rates of immigration (straight dotted arrows) are independent of local abundances.

2.2. Stochastic processes

We specify individual rates of movement, birth, and mortality in an individual-based stochastic framework, using a birth-death master equation (van Kampen 2007; Gardiner 2009). The numbers of predators and prey that inhabit a patch at any given time is governed by stochastic processes and will therefore be represented by random variables. Let X_p and X_n be discrete random variables denoting the local populations of predator and prey individuals, respectively. There can be $x_\mathrm{p} = \{0, 1, 2, ..., \infty\}$ individuals of X_p in any patch, as well as $x_\mathrm{n} = \{0, 1, 2, ..., \infty\}$ individuals of X_n in any patch. The distribution of patches with a certain combination of prey and predator numbers at time t is then defined by the joint probability distribution $D(x_\mathrm{n}, x_\mathrm{p}, t)$. The expectation (average) of any function $f(X_\mathrm{n}, X_\mathrm{p})$ is denoted with angular brackets such that $\langle f(X_\mathrm{n}, X_\mathrm{p})\rangle = \sum_{x_\mathrm{n}} \sum_{x_\mathrm{p}} D(x_\mathrm{n}, x_\mathrm{p}, t) f(x_\mathrm{n}, x_\mathrm{p})$.

In every infinitesimally small time step, $\mathrm{d}t$, a patch can either gain one individual of either species, lose one individual of either species, or remain unchanged. Hence, apart from the case where the patch remain unchanged there are four possible one-step transitions

$$\begin{aligned}
&1.\ \ X_\mathrm{n} \to X_\mathrm{n} + 0 \text{ and } X_\mathrm{p} \to X_\mathrm{p} - 1,\\
&2.\ \ X_\mathrm{n} \to X_\mathrm{n} + 0 \text{ and } X_\mathrm{p} \to X_\mathrm{p} + 1,\\
&3.\ \ X_\mathrm{n} \to X_\mathrm{n} - 1 \text{ and } X_\mathrm{p} \to X_\mathrm{p} + 0,\\
&4.\ \ X_\mathrm{n} \to X_\mathrm{n} + 1 \text{ and } X_\mathrm{p} \to X_\mathrm{p} + 0,
\end{aligned} \tag{1}$$

where $X_\mathrm{a} \to X_\mathrm{a} + 0$ indicates that the number of individuals belonging to species a does not change. Increases in the number of individuals present within the patch are indicated by positive transition rates T^+, while losses of individuals are denoted by negative transition rates T^-. The transition rates specify the

probability per unit time, that one of the individuals in a patch will die or leave the patch, or that an individual will be born or will enter the patch. The processes that can cause the number of prey in a patch to change by one are

$$\begin{aligned}&\text{birth}: \quad bX_\mathrm{n},\\ &\text{death}: \quad dX_\mathrm{n},\\ &\text{predation}: \quad \alpha X_\mathrm{p}X_\mathrm{n},\\ &\text{emigration}: \quad E_\mathrm{n}\left(X_\mathrm{p}\right)X_\mathrm{n},\\ &\text{immigration}: \quad \left\langle E_\mathrm{n}\left(X_\mathrm{p}\right)X_\mathrm{n}\right\rangle,\end{aligned} \tag{2}$$

where b is the prey birth rate, d is the prey death rate, and α is the predator attack rate on prey. Prey emigration and immigration are governed by the prey emigration-rate response $E_\mathrm{n}\left(X_\mathrm{p}\right)$, which depends on the number of predators X_p. The corresponding processes that can cause the number of predators in a patch to change by one are

$$\begin{aligned}&\text{birth}: \quad \eta\alpha X_\mathrm{n}X_\mathrm{p},\\ &\text{death}: \quad mX_\mathrm{p},\\ &\text{emigration}: \quad E_\mathrm{p}\left(X_\mathrm{n}\right)X_\mathrm{p},\\ &\text{immigration}: \quad \left\langle E_\mathrm{p}\left(X_\mathrm{n}\right)X_\mathrm{p}\right\rangle,\end{aligned} \tag{3}$$

where η is the conversion efficiency and m is the predator death rate. Predator emigration and immigration are governed by the predator emigration-rate response $E_\mathrm{p}\left(X_\mathrm{n}\right)$. This set of prey and predator processes defines the transition rates such that

$$\begin{aligned}T_n^+(X_\mathrm{n},X_\mathrm{p}) &= bX_\mathrm{n}+\left\langle E_\mathrm{n}\left(X_\mathrm{p}\right)X_\mathrm{n}\right\rangle,\\ T_n^-(X_\mathrm{n},X_\mathrm{p}) &= \alpha X_\mathrm{p}X_\mathrm{n}+dX_\mathrm{n}+E_\mathrm{n}\left(X_\mathrm{p}\right)X_\mathrm{n}\\ T_p^+(X_\mathrm{n},X_\mathrm{p}) &= \eta\alpha X_\mathrm{n}X_\mathrm{p}+\left\langle E_\mathrm{p}\left(X_\mathrm{n}\right)X_\mathrm{p}\right\rangle,\\ T_p^-(X_\mathrm{n},X_\mathrm{p}) &= mX_\mathrm{p}+E_\mathrm{p}\left(X_\mathrm{n}\right)X_\mathrm{p}.\end{aligned} \tag{4}$$

These processes drive the predator-prey dynamics and cause the distribution $D(x_\mathrm{n},x_\mathrm{p},t)$ to change over time. The dynamics of $D(x_\mathrm{n},x_\mathrm{p},t)$ are described by a birth-death master equation:

$$\begin{aligned}&\frac{\mathrm{d}D(x_\mathrm{n},x_\mathrm{p})}{\mathrm{d}t}=\\ &D(x_\mathrm{n}+1,x_\mathrm{p})T_n^-(x_\mathrm{n}+1,x_\mathrm{p})+D(x_\mathrm{n}-1,p)T_n^+(x_\mathrm{n}-1,x_\mathrm{p})\\ &+D(x_\mathrm{n},x_\mathrm{p}+1)T_p^-(x_\mathrm{n},x_\mathrm{p}+1)+D(x_\mathrm{n},x_\mathrm{p}-1)T_p^+(x_\mathrm{n},x_\mathrm{p}-1)\\ &-D(x_\mathrm{n},x_\mathrm{p})\big(T_n^-(x_\mathrm{n},x_\mathrm{p})+T_n^+(x_\mathrm{n},x_\mathrm{p})+T_p^-(x_\mathrm{n},x_\mathrm{p})+T_p^+(x_\mathrm{n},x_\mathrm{p})\big).\end{aligned} \tag{5}$$

The notation of time is dropped here for the sake of brevity. A general presentation of this equation is given in Appendix A.

2.3. Emigration-rate responses

We assume that the emigration-rate responses are the sum of two parts: density-independent movements and density-dependent movements. Specifically,

$$\begin{aligned}E_\mathrm{n}\left(X_\mathrm{p}\right) &= I+\hat{E}_\mathrm{n}(X_\mathrm{p})\\ E_\mathrm{p}\left(X_\mathrm{n}\right) &= I+\hat{E}_\mathrm{p}(X_\mathrm{n}),\end{aligned} \tag{6}$$

where I is the density independent movement component and $\hat{E}_\mathrm{n}(X_\mathrm{p})$ and $\hat{E}_\mathrm{p}(X_\mathrm{n})$ are the density-dependent movement components in which a parameter θ sets the degree of density dependence. Thus, I is a constant and the density-dependent movement components are functions that are dependent on heterospecific densities. Because prey tend to avoid predators and predators are attracted to prey ($E_\mathrm{n}'\left(X_\mathrm{p}\right)>0$ and $E_\mathrm{p}'\left(X_\mathrm{n}\right)<0$), we identify four fundamental shapes of emigration rate responses (figure 2), which will be further analyzed in the results section.

3. Results

We now show how density-dependent movements affect the spatial distributions of predators and prey, and thus the intensity and stability of their interactions. The critical properties of the system are the shapes of the density dependent emigration-rates and we derive simple criteria that link the shapes of these responses to the stability of the predator-prey dynamics and to the outcome of the space race. These general criteria are then used to analyze the stability of 16 fundamental types of interactions, which are based on the shapes of the emigration responses (figure 2). Finally we analyze published studies of emigration rate responses in order to evaluate which of the 16 types of interactions that are commonly found in empirical systems.

3.1. How density-dependent movements affect the interactions between predators and prey

The global dynamics of the system are defined by the spatial means of the local processes specified in eq. (5). Hence, as we show in Appendix B, the predator mean $P=\langle X_\mathrm{p}\rangle$ and the prey mean $N=\langle X_\mathrm{n}\rangle$ evolve over time as follows:

$$\begin{aligned}\frac{\mathrm{d}N}{\mathrm{d}t} &= rN-\alpha NP-\alpha\ \mathrm{cov}(X_\mathrm{n},X_\mathrm{p})\\ \frac{\mathrm{d}P}{\mathrm{d}t} &= \eta\alpha NP-mP+\eta\alpha\ \mathrm{cov}(X_\mathrm{n},X_\mathrm{p}).\end{aligned} \tag{7}$$

The Lotka-Volterra predator-prey model is recovered, with the addition of the spatial covariance $\mathrm{cov}(X_\mathrm{n},X_\mathrm{p})$ between predator and prey. A negative covariance indicates that predators and prey tend to occupy different spatial regions, while a positive covariance indicates that they tend to occupy the same regions. This means for an individual predator (or a prey) that it will experience either fewer or more encounters with prey individuals (or predator individuals) than would be expected based exclusively on the mean density of each species in the system. This is statistically described by the per capita covariance

$$C=\frac{\mathrm{cov}\left(X_\mathrm{n},X_\mathrm{p}\right)}{NP}, \tag{8}$$

which allows us to reformulate eq. (7) in a simplified form

$$\begin{aligned}\frac{\mathrm{d}N}{\mathrm{d}t} &= rN-\alpha NP(1+C)\\ \frac{\mathrm{d}P}{\mathrm{d}t} &= \eta\alpha NP(1+C)-mP.\end{aligned} \tag{9}$$

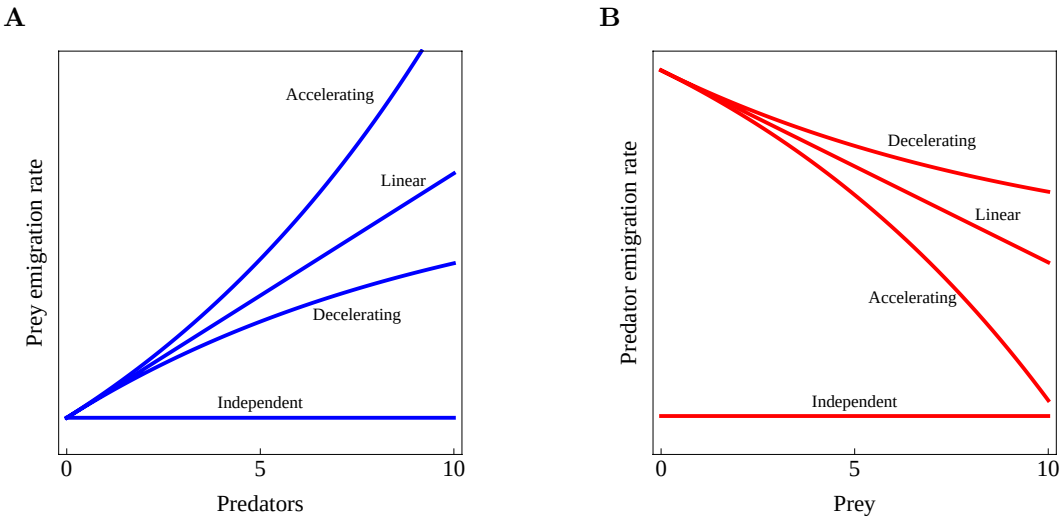

Figure 2: Four fundamental types of emigration-rate responses of prey (**A**) and predators (**B**).

Thus, C can be interpreted as a reaction-rate correction, which corrects the assumption that individuals follow the law of mass action. We show in Appendix B that the per capita covariance arising from density-dependent movement processes is approximated by

$$C \approx -\frac{E'_{\mathrm{n}}(P) + E'_{\mathrm{p}}(N)}{E_{\mathrm{n}}(P) + E_{\mathrm{p}}(N)}, \tag{10}$$

where $E_{\mathrm{n}}(P)$ and $E_{\mathrm{p}}(N)$ are the emigration-rate responses of the prey and the predator, respectively. Strictly speaking, this approximation is only valid when the density dependence of the movement processes is weak. However, numerical investigations (Appendix D) show that this approximation remains valid in the range of degrees of density dependence that are typically observed in nature (Table 1).

The per capita covariance can be used to predict what happens when the prey is repelled by predators and predators are attracted to prey. It also describes how the environment is perceived by individuals. The abundance of prey perceived by the average predator is $N(1+C)$; symmetrically, the predator abundance perceived by the average prey is $P(1+C)$.

Figure 3 exemplifies how per capita covariances may depend on densities and the shapes of the emigration rate responses. The per capita covariance surface shown in figure 3A represents a case in which the prey has an accelerating emigration-rate response to predators while the predator has a decelerating emigration-rate response to prey, as shown in figure 3C. This combination of responses is frequently found in empirical studies (see section *Empirical emigration-rate responses*). Figure 3B shows the per capita covariance surface for a situation in which both the prey and the predator have decelerating emigration-rate responses, as shown in figure 3D. The surfaces have domains of positive or negative per capita covariances, which are equivalent to positive and negative correlations, respectively. A positive correlation ($E'_{\mathrm{n}}(P) < -E'_{\mathrm{p}}(N)$) means that the predator is "winning" the space-race in the sense that it is better at tracking the prey than the prey is at avoiding predators. A negative correlation ($E'_{\mathrm{n}}(P) > -E'_{\mathrm{p}}(N)$) means the opposite. There are consequently lines of zero covariance (i.e. zero correlation), which correspond to cases in which both species are equally good at avoiding or tracking one-another. Under such conditions, the absolute value of the slopes of the two species' emigration-rate responses are equal and so the two species are equally good at adjusting their spatial position based on the local abundance of the other.

3.2. The effects of density-dependent movements on demographic stability

The demographic stability of the large-scale predator-prey system (eq. 7) is determined by analysing the Jacobian matrix for the system at equilibrium. The equilibrium densities of the non-spatial Lotka-Volterra model are well known; the prey equilibrium is $m/(\alpha\eta)$ and the predator equilibrium is r/α. We can solve the spatial Lotka-Volterra model (eq. 9) to determine its pseudo-equilibrium densities, which are found to depend on the per capita covariance between predators and prey such that

$$\begin{aligned} N^* &= \frac{m}{\alpha\eta}\frac{1}{(1+C)} \\ P^* &= \frac{r}{\alpha}\frac{1}{(1+C)}. \end{aligned} \tag{11}$$

C is bounded between -1 and infinity for non-negative densities. As $C \to -1$, the equilibrium densities approach infinity. When $C = 0$, the equilibrium densities are equal to those expected according to the non-spatial model, and as $C \to \infty$, the equilibrium densities approach zero. While this is interesting in and of itself, our model is analyzed when the density dependence of dispersal is weak. Under such conditions, C is close to zero why the equilibrium densities should be near those of the classic non-spatial Lotka-Volterra model.

When investigating the stability of eq. (9) we assume that the system is at its fixed points and then determine whether a given set of statements are true or false for all $N = N^* > 0$ and $P = P^* > 0$. In Appendix C we show that the stability of the predator-prey system is determined by the shape of the

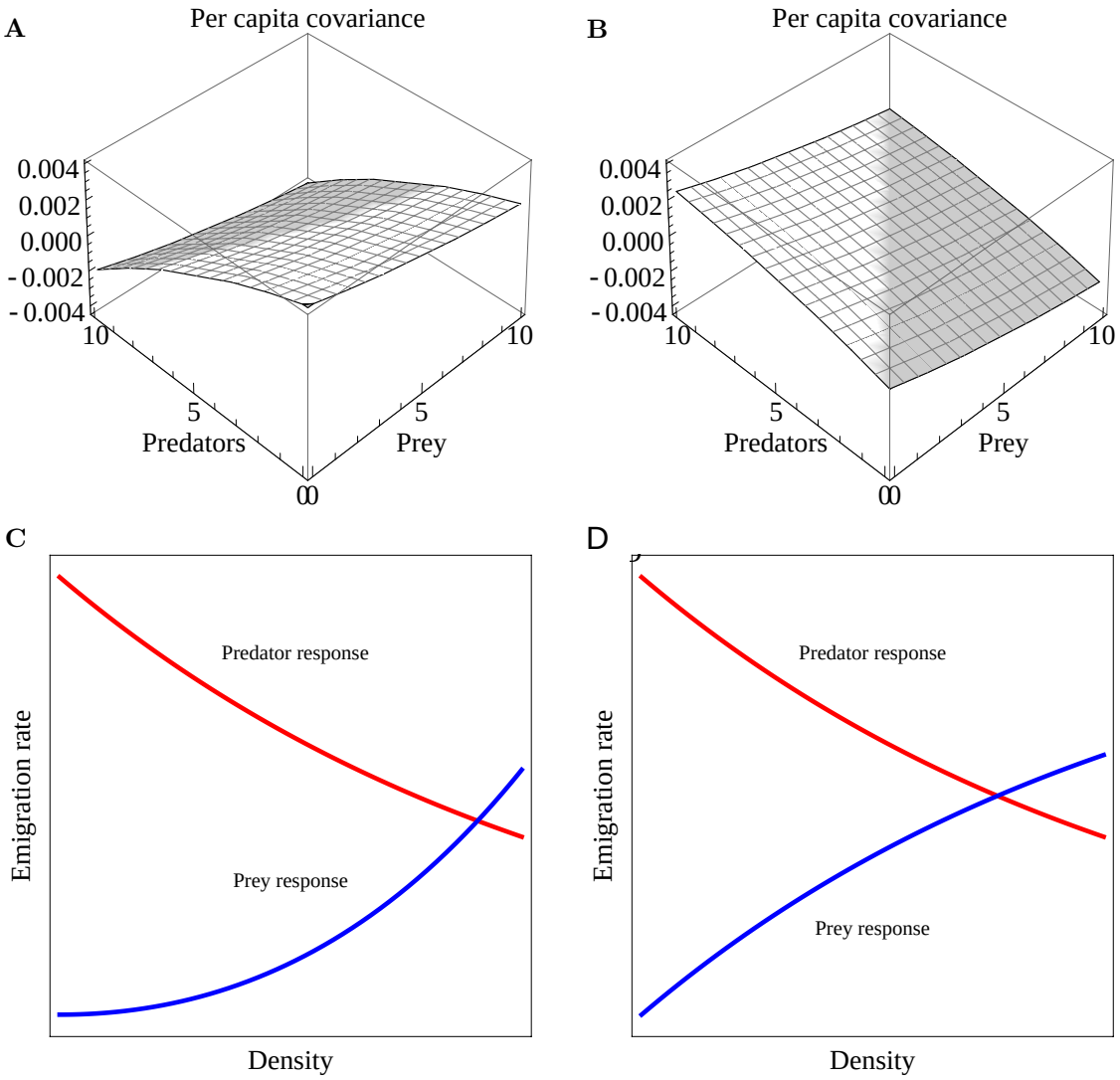

Figure 3: **A** depicts the per capita covariance surface produced when prey have an accelerating emigration-rate response to predators and the predators have a decelerating emigration response to prey, as shown in **C**, whereas **B** depicts the per capita covariance surface produced when both the prey and the predator have decelerating emigration-rate responses, as shown in **D**. The per capita covariance surfaces have positive (light) and negative (dark) domains. The per capita covariance is positive when the predator's emigration-rate response is steeper than that of the prey. The opposite is true when the per capita covariance is negative.

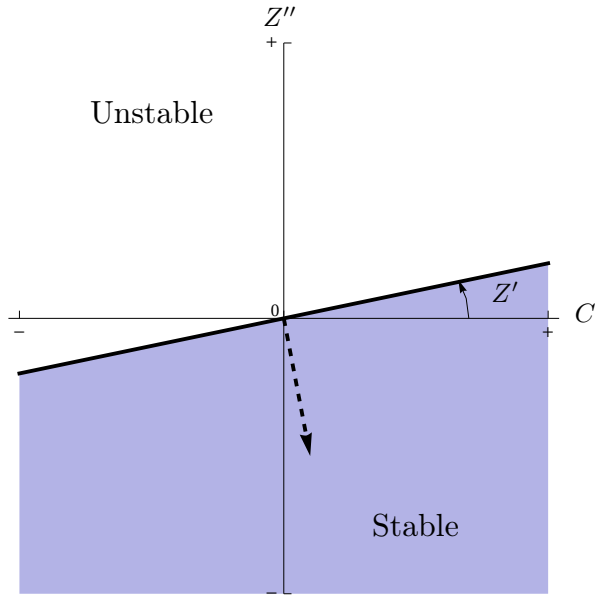

Figure 4: A graphical representation of the effects of density-dependent movements on the stability of predator-prey dynamics. In the (C, Z'')-plane, the stability is determined by the per capita covariance C and the non-linearity term Z''. The "angle" of the boundary $Z'' = Z'C$ (black line) is determined by Z'. This affects the "stabilizing direction" (dashed arrow) in the (C, Z'')-plane. Hence, small values of Z'' and large values of C are stabilizing. The sign of C determines the "stabilizing direction" of Z'. If $C > 0$ then an increasing Z' is stabilizing, whilst if $C < 0$ then a decreasing Z' is stabilizing.

per capita covariance and the conversion efficiency, such that fixed points that satisfy

$$\eta \frac{\partial C}{\partial P} < \frac{\partial C}{\partial N}, \tag{12}$$

are stable (attractors), or are otherwise unstable (repellers). We can therefore determine the stability of a system by examining the slopes of its per capita covariance. For instance, we can tell that figure 3A represents a stable system and that figure 3B represents an unstable system (assuming that $\eta \approx 1$ and that the fixed point lies within the visible surfaces).

Since the shape of the per capita covariance is governed by the emigration-rate responses it is also of interest to investigate closer the stabilising properties of the emigration-rate responses themselves. Eq. (12) can be reduced to

$$E_{\mathrm{p}}'' - \eta E_{\mathrm{n}}'' - C\left(\eta E_{\mathrm{n}}' - E_{\mathrm{p}}'\right) < 0, \tag{13}$$

where we have used the short notation: $E_{\mathrm{n}} = E_{\mathrm{n}}(P^*)$ and $E_{\mathrm{p}} = E_{\mathrm{p}}(N^*)$. If eq. (13) is true, the system is stable (Appendix C). We see that it is the first and second order derivatives of the emigration-rate responses that govern the stability of the system, and that the prey's response is weighted by η.

Eq. (13) can be simplified and expressed in a "categorical" form

$$Z'' - Z'C < 0, \tag{14}$$

where $Z'' = E_{\mathrm{p}}'' - \eta E_{\mathrm{n}}''$ is the contribution from the non-linearities of the emigration-rate responses, $Z' = -E_{\mathrm{p}}' + \eta E_{\mathrm{n}}' > 0$ is a measure of the relative steepness of the emigration-rate responses, and C is the per capita covariance (Appendix C).

Figure 4 illustrates how the stability of the predator-prey dynamics is affected by density-dependent movements. The general conclusion to be drawn from this figure is that there are three routes to stability that depend on the sizes of Z'', Z', and C: (1) A small non-linearity term Z'' is stabilizing, from which it follows that large values of E_{n}'' and small values of E_{p}'' are stabilizing, and; (2) a large per capita covariance C is stabilizing, which means that positively small values of E_{n}' and negatively large values of E_{p}' are stabilizing, and; (3) large values of Z' is stabilizing if $C > 0$ and destabilising if $C < 0$.

We can also identify two special cases in which the stability criteria become more simple: First, when the emigration-rate responses are linear ($Z'' = 0$), the stability of the system depends only on the per capita covariance (Z' is just a positive coefficient), and the system is stable if

$$C > 0, \tag{15}$$

which in this case is equivalent to saying that the spatial correlation between predators and prey is positive. This happens if the predator is "winning" the space-race. Therefore, if the predators' tracking-efficiency is greater than the prey's efficiency of avoidance, we can express this case as follows in terms of emigration-rate responses: $-E_{\mathrm{p}}' > E_{\mathrm{n}}'$. Second, if the non-linearities are non-zero ($Z'' \neq 0$), while the density independent movement component (I) is very large, the contribution of the per capita covariance becomes negligible because I is represented in the denominator of C. In this case, the stability of the system depends only on the non-linearities of the emigration-rate responses such that the system is stable if

$$Z'' < 0, \tag{16}$$

In terms of the emigration-rate responses, this is equivalent to saying that the second derivative of the predator's emigration-rate response is smaller than that of the prey weighted by η, hence, $E_{\mathrm{p}}'' < \eta E_{\mathrm{n}}''$.

3.3. The stability of 16 specific types of predator-prey movement behaviors

In section *Emigration-rate responses* we identified four basic shapes of emigration responses: independent, linear, decelerating and accelerating responses. These shapes can be combined to define 16 fundamental types of space-races that differ in their effects on stability. In figure 5 we present, for each of the 16 types, the effects of movements on stability, by evaluating eq. (14) when the density-dependent movement component is small relative to the independent movement component.

Critical for stability under this assumption is the sign of Z'' or, if Z'' is zero, the sign of the per capita covariance C. One important special case occurs when both species move independently of each other (figure 5A). The neutrally stable Lotka-Volterra system is then recovered. A second case, shown in

Table 1: Emigration-rate responses of prey and predators reported in published studies.

Study	Predator	Prey	Response	Slope	Shape	θ
Bernstein (1984)	Mite (*Phytoseiulus*)	Mite (*Tetranychus*)	Predator	−	Decelerating	0.11
French and Travis (2001)	Wasp (*Anisopteromalus*)	Beetle (*Callosobruchus*)	Predator	−	Decelerating	0.0013
Hauzy et al. (2007)	Protist (*Dileptus*)	Protist (*Tetrahymena*)	Predator	−	Decelerating	0.0002
Jenner and Roitberg (2008)	Wasp (*Campoplex*)	Moth (*Enarmonia*)	Predator	−	Decelerating	0.51
Kratz (1996)	Stonefly (*Doroneuria*)	Mayfly (*Baetis*)	Predator	−	Decelerating	0.0023
Maeda et al. (1998)	Mite (*Phytoseiulus*)	Mite (*Tetranychus*)	Predator	−	Decelerating	0.012
Nachappa et al. (2006)	Mite (*Phytoseiulus*)	Mite (*Tetranychus*)	Predator	−	Decelerating	0.31
Ohara and Takabayashi (2012)	Wasp (*Diadegma*)	Moth (*Plutella*)	Predator	−	Decelerating	0.072
Roll et al. (2004)[a]	Mayfly (*Baetis*)	Periphyton	Predator	−	Decelerating	NA
Roll et al. (2004)[b]	Mayfly (*Baetis*)	Periphyton	Predator	−	Decelerating	NA
Zemek and Nachman (1998)	Mite (*Phytoseiulus*)	Mite (*Tetranychus*)	Predator	−	Decelerating	0.034
Hassell (1971)	Wasp (*Nemeritis*)	Moth (*Ephestia*)	Predator	−	Decelerating	0.017
Bernstein (1984)	Mite (*Phytoseiulus*)	Mite (*Tetranychus*)	Prey	+	Linear/Accelerating	0.032
Diehl et al. (2000)	Fish (*Salmo*)	Mayfly (*Baetis*)	Prey	+	Accelerating	0.0056
Forrester (1994)[c]	Fish (*Salvelinus*)	Mayfly (*Baetis*)	Prey	+	Linear/Accelerating	0.46
Forrester (1994)[c]	Fish (*Salvelinus*)	Mayfly (*Paraleptophlebia*)	Prey	+	Accelerating	0.36
Forrester (1994)[d]	Fish (*Salvelinus*)	Mayfly (*Baetis*)	Prey	+	Accelerating	1.24
Hauzy et al. (2007)	Protist (*Dileptus*)	Protist (*Tetrahymena*)	Prey	+	Accelerating	0.0095

[a]Large *Baetis* 1995 experiment.
[b]Small *Baetis* 1996 experiment.
[c]2 m patches.
[d]Stream section.

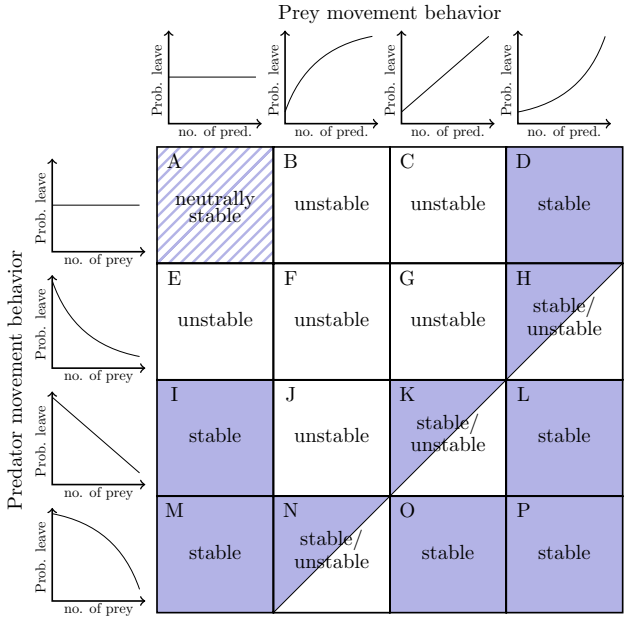

Figure 5: Effects of different emigration-rate responses on the stability of global dynamics. Stability is evaluated under conditions where the density-dependence is weak and the independent-movement component is large. Plots on the edge of the matrix show the emigration-rate responses of prey (columns) and predators (rows). The vertical axis of each plot shows the probability per unit time that an individual of the reactive species will leave its current patch, while the horizontal axes show the number of individuals of the species to which it reacts.

figure 5H, corresponds to the emigration responses most often found in empirical studies (see next section). Here the emigration responses are accelerating for prey and decelerating for predators which may stabilize or destabilize dynamics depending on the magnitudes of the second derivatives (eq. 16); a more non-linear response of the prey will tend to stabilize dynamics, whereas a more strongly decelerating response of predators will destabilize dynamics.

Note that only the first and second-order derivatives of the emigration-rate responses need to be considered when analyzing stability. This is because when the density-dependence in movements are weak, the higher order terms add only negligible amounts of information on the spatial structure (Appendix B).

3.4. Empirical emigration-rate responses

Because the shapes of the emigration-rate responses are critical for stability, it was considered important to investigate emigration-rate responses in empirical systems. We surveyed the literature for studies that reported statistically significant emigration responses of predators or prey as functions of heterospecific densities. We did not include responses that were not statistically significant because it was often impossible to determine whether the results reported in such cases reflected an absence of a response or low statistical power. In general, the experimental predator emigration-rate responses to increasing prey densities are decelerating (table 1). Prey emigration-rate responses are more variable, although accelerating responses seem to be predominant. This combination of responses typically leads to unstable dynamics (see second row in figure 5). The only exception to this general rule occurs when the prey has an accelerating response and the per capita covariance is not strongly negative.

The degree of density dependence, $\theta = |c|$, in Table 1, was estimated by fitting an exponential model of the form $a + be^{cx}$,

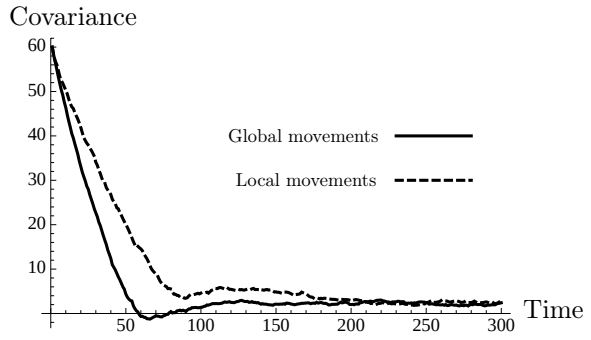

Figure 6: Results of spatially explicit simulations showing the evolution of the covariance arising from local movements (dashed line) and global movements (solid line) over time. At time zero, all 60 individuals (30 predators and 30 prey) reside in one central patch. Individuals then disperse between patches. In this example, the probability that a prey individual will leave a patch increases linearly with the number of predators, while the probability that a predator individual will leave a patch has an inverse exponential dependence on the abundance of prey.

where x is the local numbers of predators or prey. In the majority of cases (Hassell 1971; Bernstein 1984; Kratz 1996; Maeda et al. 1998; Zemek and Nachman 1998; Diehl et al. 2000; French and Travis 2001; Hauzy et al. 2007; Ohara and Takabayashi 2012), were the strength of the observed density dependence within the range for which our covariance approximation is accurate.

4. Robustness

4.1. Covariance approximation

As we explain in Appendix B the accuracy of the approximation depends on the parameter θ, which determines the steepness as well as the level of non-linearity of the emigration-rate responses, and thereby the degree of density dependence in emigration rates. By restricting the movement functions E to a confined class of functions, we show in Appendix B.3 specifically that the relative error vanishes as θ becomes small. In Appendix D, we provide results on numerical analysis supporting our analytical findings.

4.2. Global movement versus local movement

So far we have assumed that movements are global, i.e. that emigrating individuals have the same likelihood of entering all patches. A more realistic assumption is that movements are local in the sense that emigrating individuals move to patches that are adjacent to the one they currently occupy. Although the transient probability distributions produced by global and local movements are different, intuition suggests that the stationary probability distributions of global and local movement should be identical as long as the spatial network is homogeneous.

We thus expect that the covariances arising from the two different movement processes will be equivalent once a stationary state is reached. We have not been able to prove this analytically, but spatially explicit simulations support our intuition. Figure 6 shows that the spatial covariance produced by global and local movements initially follow different trajectories but soon converge. Each of the trajectories shown in the figure is an average of 40 simulations run using identical settings (15 patches arranged in a circular network) and initial conditions (all simulations were started with 30 prey individuals and 30 predator individuals in one central patch, while all of the other patches were unoccupied).

5. Discussion

This paper presents an analytical modeling framework for investigating the relationship between large scale predator-prey dynamics and small-scale density-dependent movements. We use a second order moment closure model, which is a deterministic approximation of an individual-based stochastic system. An important assumption in the model is that movement rates are much higher than vital rates, which provides the technical benefit that the direct contribution of vital processes to the spatial distribution of individuals is negligible. Under this assumption, movements rapidly drive the spatial distribution to an equilibrium, at which the full dynamical model is evaluated. The global dynamics produced by the model are highly sensitive to the assumptions made regarding movement behaviors. If all individuals move randomly, the spatial structure of the system collapses to a Poisson distribution, leading to mean-field dynamics. However, if movements are density-dependent, spatial correlations between predators and prey will emerge. These correlations may stabilize or destabilize the large scale dynamics depending on the shape of the emigration-rate responses.

The shape of emigration-rate responses should reflect the fitness consequences of either staying in a patch or searching for a better one. This problem has been studied extensively in behavioral ecology; one general conclusion of these studies has been that an organism should leave a patch only if the expected fitness is higher for emigrants than for residents (Charnov 1976; Brown 1988). The response of a single individual could thus be described by a step function, e.g. a prey individual should stay if predator densities are low, and leave if densities exceed a critical value. If rules of this sort are scaled up and applied to a population of non-identical individuals that require some time to sample heterospecific densities and that make sampling errors, one obtains sigmoidal response functions that describe the emigration rate. However, empirical data indicate that predators have decelerating emigration-rate responses to prey densities, whereas prey usually have accelerating responses (table 1). The reason for this discrepancy is not yet understood.

The effect of decelerating predator responses is destabilizing, whereas accelerating prey responses are stabilizing. The net effect will therefore depend on the relative curvature of the two responses. An understanding of the effects of density-dependent movements on stability can be obtained by considering how local movement processes induce population-level density dependencies. In this context, it is useful to consider the slope of the emigration-rate response because it determines the ability to discriminate between high and low density patches. For example, an accelerating prey emigration-rate response means that the ability of prey to discriminate between safe and dangerous patches is low when overall predator densities are low but becomes better at high predator densities. Prey are thus more efficient at avoiding predators at high predator densities, which leads to a negative and stabilizing density dependence

in predator intake rates. An analogous argument can be used for decelerating predator responses: the response function is steepest at low prey densities, which means that predators are more efficient in locating prey-rich patches when overall prey density is low. This mechanism creates a destabilizing density dependence that affects prey mortality.

A variety of modeling approaches have been used to study how movements influence predator-prey dynamics. An approach closely related to ours was used by Murdoch and Stewart-Oaten (1989) to examine the effects of within-season (small-scale) aggregation of parasitoids. Although there are important differences between the two approaches (notably, Murdoch and Stewart-Oaten (1989) use assumed spatial patterns rather than deriving them from movement rules), they do share general principles such as the assumption of a very large number of patches and the use of statistical representations of spatial patterns, suggesting that it is meaningful to compare the outputs of the two models. Murdoch and Stewart-Oaten (1989) found that stability depends on the shape of the predator aggregation response to prey densities. Specifically, for a randomly distributed host population, they show that the population dynamics are stabilized when the aggregation response of predators is stronger than linear, and destabilized if the response is weaker than linear. Our findings are consistent with these results (see the first column in figure 5 and note that the correspondence between the two models arises because accelerating movements create stronger than linear aggregation while decelerating movements lead to weaker than linear aggregation).

The paper by Murdoch and Stewart-Oaten (1989) inspired a discussion of the role of within- and between season aggregation, which is analogous to small- and large-scale movements (Godfray and Pacala 1992; Rohani et al. 1994). Assumptions about spatial scale are crucial in spatial models, and it is convenient to classify the "scale" of models based on the magnitude of movement rates relative to vital rates. The assumption that movement rates are much greater than vital rates, which was used in this study, implies that the patches are small relative to the movement capacity of the organisms (Englund and Hambäck 2004). Models assuming this type of time scale separation should thus be classified as "small scale". Such models can be contrasted with models that assume "limited movement", i.e. that movement rates are of the same magnitude as vital rates. Keeling et al. (2002) formulated moment equation models for systems with limited movement using a framework similar to ours. They assumed independent movement and found that the system is stabilized if predators move approximately six times faster than the prey. In our formulation, independent movements do nothing but recover mean-field dynamics. This demonstrates that there are two general cases in which movement or factors affecting movement can perturb a system away from the Poissonian state; the first occurs when movements are density-dependent and the second occurs when movement is limited. Limitations on movement restrict the mixing of individuals in space, thereby allowing the formation of spatial correlations. In this case, it is the combination of independent movements and stochastic birth and death processes that generates spatial heterogeneity. Conversely, in cases involving density-dependent movement, it is the movements alone that give rise to spatial heterogeneity.

As we have shown, the stability of the predator-prey system depends crucially on the shapes of the emigration-rate responses of the two species. Empirical observation (table 1) show that prey generally have an accelerating emigration-rate response to predators while predators have a decelerating emigration-rate response to prey. The accelerating response stabilizes the dynamics of the system whereas the decelerating response has a destabilizing effect. The relationship between the two responses thus determines the stability of the predator-prey system. It therefore follows that in order to predict the dynamics of a coupled prey and predator species, it is essential to understand the relationship between the two species' emigration-rate responses. However, the majority of the existing empirical data (table 1) concerns either the prey response alone or the predator response alone. As such, there is a need for new studies on coupled small-scale emigration-rate responses of predators and prey in order to determine whether density-dependent movements generally have stabilizing or destabilizing effects on predator-prey dynamics.

A problem that may arise when using moment approximations is that the rates of the studied processes directly affect the accuracy of the approximation. For instance, Keeling et al. (2002) evaluated the dynamical effects of limited movement rates by decreasing these rates. However, this violates the approximation and at some point, the model will break down. To some extent, this problem can be ameliorated by including higher order moments. The same phenomenon occurs in our model in the sense that the strength of reactivity, i.e. the slopes and non-linearities of the emigration-rate responses, must be small for the approximation to hold. However, the general shapes of the functions do not affect the accuracy of the approximation, suggesting that the disregard of higher order moments does not have severe consequences. Perhaps more critical, though, is the simplifying assumption that global movements are effectively equivalent to local movements in the ergodic state of the system. The assumption is powerful in the sense that it substantially reduces the complexity of the master equation. Although supported by intuition and numerical simulations, a rigorous proof of this assumption would be beneficial for the future development of this framework.

Dieckmann and Law (2001) noted that "theory in spatial ecology has to steer a narrow and challenging course between the Scylla of oversimplification and the Charybdis of intractability". We have formulated a spatio-temporal predator-prey model that describes how predator and prey individuals simultaneously react to local numbers of heterospecifics and subsequently relocate themselves according to explicit movement rules. The model incorporates important components of natural systems, such as stochasticity and a large number of patches, while remaining analytically tractable. A limitation is that the deterministic approximation is theoretically only valid in the Poisson limit, i.e. when the density dependence in emigration responses is weak. However, our robustness analysis shows that the approximation error in our model is negligible if the strength of the density dependent emigration functions corresponds to that typically observed in empirical studies. Stronger density dependence, which would require higher-order approximation, was observed in only one case (Forrester 1994). This suggests that our deterministic approximation is valid for modelling the spatial density-dependent processes that are captured at scales at which the processes are typically studied. To reach confidence, however, it will important to investigate the density dependence of emigration responses in a wider range of natural systems.

Acknowledgments

We want to thank Jun Yu and Zhenqing Li for discussions during early stages of the work, Etsuko Nonaka for comments on a previous draft of this article, and Mats Bodin as well as Klas Markström for good advice. G. E. and H. S. were supported by a grant from the Swedish Research Council.

Appendix A. Multivariate birth death master equation

The master equation is derived on the general assumption of Q species in a spatial domain. However, please note that for the purpose of this paper, $Q = 2$ is sufficient. The spatial domain is divided into an infinite number of sub-domains, or patches. In any and every patch, at a given point in time, there are $\mathbf{X} = \{X_1, X_2, \ldots, X_Q\}$ individuals of species $\{1, 2, \ldots, Q\}$, and all X may take on any non-negative discrete number x in a stochastic fashion. Therefore, at every point in time, each patch occupies a state $\mathbf{x} = (x_1, x_2, \ldots, x_Q)$ that is defined by the number of individuals from each of the Q species within that patch. We introduce the discrete probability distribution $D(\mathbf{x}, t)$, which describes the relative number of spatial patches that are in the state $\mathbf{x}$ at time t. The patch-states will change over time due to stochastic processes (T), and the time evolution of $D(\mathbf{x}, t)$ is described by the master equation

$$\begin{aligned}\frac{\mathrm{d}D(\mathbf{x},t)}{\mathrm{d}t} = \sum_{A=1}^{Q} \Big[& D(x_A+1,\hat{\mathbf{x}},t)T_A^-(x_A+1,\hat{\mathbf{x}}) \\ & + D(x_A-1,\hat{\mathbf{x}},t)T_A^+(x_A-1,\hat{\mathbf{x}}) \\ & - D(\mathbf{x},t)\big(T_A^-(\mathbf{x}) + T_A^+(\mathbf{x})\big)\Big],\end{aligned} \tag{A.1}$$

where the function T_A^- denotes transition processes that promote negative changes ($X_A \to X_A - 1$) in X_A. Similarly, the function T_A^+ denotes transition processes that promote positive changes ($X_A \to X_A + 1$) in X_A. $\hat{\mathbf{x}}$ is a notation for a vector with all x except x_A.

Appendix B. Moment function, global dynamics and covariance approximation

Appendix B.1. Moment function

We assume, as in Appendix A, a general system of Q species, and note that $Q = 2$ applies to the predator-prey system under consideration in this paper.

The expectation of any function $f(\mathbf{X})$ where $\mathbf{X} = (X_1, X_2, \ldots, X_Q)$ and all X are discrete random variables can be denoted by angular brackets such that

$$\langle f(\mathbf{X}) \rangle = \sum_{x_1} \sum_{x_2} \cdots \sum_{x_Q} D(\mathbf{x}) f(\mathbf{x}), \tag{B.1}$$

where $D(\mathbf{x})$ is the probability distribution of $\mathbf{X}$. Consider then the central moment

$$\begin{aligned}&\left\langle \prod_{A=1}^{Q} (X_A - \langle X_A \rangle)^{\lambda_A} \right\rangle = \\ &\sum_{x_1=0}^{\infty} \sum_{x_2=0}^{\infty} \cdots \sum_{x_Q=0}^{\infty} \left[D(\mathbf{x},t) \prod_{A=1}^{Q} (x_A - \langle X_A \rangle)^{\lambda_A} \right]\end{aligned} \tag{B.2}$$

for components $\{X_1, X_2, \ldots, X_Q\}$, where λ_A denotes the Ath component's contribution to the moment. Since the probability distribution $D(\mathbf{x}, t)$ (Appendix A) is unknown, we cannot solve eq. (B.2) for the central moment directly. However, the processes (eq. A.1) that give rise to $D(\mathbf{x}, t)$ are known, so we may express the time evolution of eq. (B.2)

$$\begin{aligned}&\frac{\mathrm{d}}{\mathrm{d}t} \left\langle \prod_{A=1}^{Q} (X_A - \langle X_A \rangle)^{\lambda_A} \right\rangle = \\ &\sum_{x_1=0}^{\infty} \sum_{x_2=0}^{\infty} \cdots \sum_{x_Q=0}^{\infty} \left[\frac{\mathrm{d}D(\mathbf{x},t)}{\mathrm{d}t} \prod_{A=1}^{Q} (x_A - \langle X_A \rangle)^{\lambda_A} \right] = \\ &\sum_{x_1=0}^{\infty} \sum_{x_2=0}^{\infty} \cdots \sum_{x_Q=0}^{\infty} \Big[\sum_{A=1}^{Q} \Big(D(x_A+1,\hat{\mathbf{x}},t)T_A^-(x_A+1,\hat{\mathbf{x}}) \\ &+ D(x_A-1,\hat{\mathbf{x}},t)T_A^+(x_A-1,\hat{\mathbf{x}}) \\ &- D(\mathbf{x},t)\big(T_A^-(\mathbf{x}) + T_A^+(\mathbf{x})\big)\Big) \prod_{A=1}^{Q} (x_A - \langle X_A \rangle)^{\lambda_A} \Big]\end{aligned} \tag{B.3}$$

and after simplification, we find that

$$\begin{aligned}&\frac{\mathrm{d}}{\mathrm{d}t} \left\langle \prod_{A=1}^{Q} (X_A - \langle X_A \rangle)^{\lambda_A} \right\rangle = \\ &= \sum_{x_1=0}^{\infty} \sum_{x_2=0}^{\infty} \cdots \sum_{x_Q=0}^{\infty} \Big[D(\mathbf{x},t) \\ &\times \sum_{A=1}^{Q} \Big(T_A^-(\mathbf{x}) \Big((x_A - 1 - \langle X_A \rangle)^{\lambda_A} \prod_{\hat{B}=1}^{Q} (x_{\hat{B}} - \langle X_{\hat{B}} \rangle)^{\lambda_{\hat{B}}} \\ &- \prod_{B=1}^{Q} (x_B - \langle X_B \rangle)^{\lambda_B} \Big) \\ &+ T_A^+(\mathbf{x}) \Big((x_A + 1 - \langle X_A \rangle)^{\lambda_A} \prod_{\hat{B}=1}^{Q} (x_{\hat{B}} - \langle X_{\hat{B}} \rangle)^{\lambda_{\hat{B}}} \\ &\prod_{B=1}^{Q} (x_B - \langle X_B \rangle)^{\lambda_B} \Big) \Big) \Big],\end{aligned} \tag{B.4}$$

where $\hat{B}$ is an index of all x exempt for x_A. After further simplification we have

$$\frac{\mathrm{d}}{\mathrm{d}t}\left\langle \prod_{A=1}^{Q}(X_A-\langle X_A\rangle)^{\lambda_A}\right\rangle =$$
$$=\left\langle \sum_{A=1}^{Q}\left[T_A^-(\mathbf{X})\left(\frac{(X_A-1-\langle X_A\rangle)^{\lambda_A}}{(X_A-\langle X_A\rangle)^{\lambda_A}}\prod_{B=1}^{Q}(X_B-\langle X_B\rangle)^{\lambda_B}\right)\right.\right.$$
$$+T_A^+(\mathbf{X})\left(\frac{(X_A+1-\langle X_A\rangle)^{\lambda_A}}{(X_A-\langle X_A\rangle)^{\lambda_A}}\prod_{B=1}^{Q}(X_B-\langle X_B\rangle)^{\lambda_B}\right)$$
$$\left.\left.-\prod_{B=1}^{Q}(X_B-\langle X_B\rangle)^{\lambda_B}\left(T_A^-(\mathbf{X})+T_A^+(\mathbf{X})\right)\right]\right\rangle. \tag{B.5}$$

Define

$$\begin{aligned}
&\varphi(X_A)=(X_A-\mu_A)^{\lambda_A}\\
&G_A^-=T_A^-(\mathbf{X})\left(\frac{\varphi(X_A-1)}{\varphi(X_A)}-1\right)\\
&G_A^+=T_A^+(\mathbf{X})\left(\frac{\varphi(X_A+1)}{\varphi(X_A)}-1\right)\\
&\kappa=(\lambda_1,\lambda_2,\ldots,\lambda_Q)\\
&\Lambda_\kappa=\prod_{A=1}^{Q}\varphi(X_A).
\end{aligned} \tag{B.6}$$

The moment function may then be written as

$$\frac{\mathrm{d}\langle\Lambda_\kappa\rangle}{\mathrm{d}t}=\left\langle\Lambda_\kappa\sum_{A=1}^{Q}\left(G_A^-+G_A^+\right)\right\rangle \tag{B.7}$$

when letting $\mu_A=\langle X_A\rangle$. By setting the left hand side of eq. (B.7) to zero, we then can solve for the central moment $\langle\Lambda_\kappa\rangle$ at the stationary state of $D(\mathbf{x},t)$.

Appendix B.2. Generalized moment function and global dynamics

The formulation of the moment function above is explicitly for central moments. However, note that $\varphi(X_A)$ may be substituted by any arbitrary function $f(X_A)$ of species A. Then, by solving eq. (B.7) for Λ_κ, we will instead of the central moment get the expectation of $f(\mathbf{X})$ where $\mathbf{X}=(X_1,X_2,\ldots,X_Q)$. A general formulation of eq. (B.7) was implemented in the derivation of the global dynamics eq. (7), such that for $\frac{\mathrm{d}N}{\mathrm{d}t}$ we set $\varphi(X_\mathrm{n})=X_n^1$ and $\varphi(X_\mathrm{p})=X_p^0$, and for $\frac{\mathrm{d}P}{\mathrm{d}t}$ we set $\varphi(X_\mathrm{n})=X_n^0$ and $\varphi(X_\mathrm{p})=X_p^1$. Then,

$$\begin{aligned}
\frac{\mathrm{d}\langle\Lambda_{1,0}\rangle}{\mathrm{d}t}&=\frac{\mathrm{d}\left\langle X_\mathrm{n}^1X_\mathrm{p}^0\right\rangle}{\mathrm{d}t}=\frac{\mathrm{d}N}{\mathrm{d}t}\\
\frac{\mathrm{d}\langle\Lambda_{0,1}\rangle}{\mathrm{d}t}&=\frac{\mathrm{d}\left\langle X_\mathrm{n}^0X_\mathrm{p}^1\right\rangle}{\mathrm{d}t}=\frac{\mathrm{d}P}{\mathrm{d}t}.
\end{aligned} \tag{B.8}$$

Appendix B.3. Approximation error and requirements on emigration-rate functions

We assume that the emigration-rate functions E_1 and E_2 are such that they approach constant functions when θ tends to zero from above. Specifically, writing

$$E(X)=E(\mu)+E'(\mu)(X-\mu)+R(X), \tag{B.9}$$

we assume that all moments of $E(X)$, where X is a random variable for the local number of individuals of either species 1 or species 2, are of order θ^2, while $E(\mu)$ and $E'(\mu)$ where μ is the heterospecific mean density, satisfy

$$L\theta^k\le|E^{(k)}(\mu)|\le U\theta^k, \tag{B.10}$$

for $k=0$ and $k=1$, where L and U are positive constants. As an example, we assume functions $E(X)$ with properties analogous to that of $e^{\theta X}$. Finally, in order to avoid a degenerate case, which is explained further in Appendix B.4, we require in analogy with eq. (B.10) that

$$\tilde{L}\theta\le|E_1'(\mu_2)+E_2'(\mu_1)|\le\tilde{U}\theta, \tag{B.11}$$

for species 1 and 2.

We desire to obtain a covariance approximation such that the relative approximation-error

$$\epsilon=\frac{\epsilon_\mathrm{abs}}{\mathrm{cov}(X_1,X_2)}, \tag{B.12}$$

where the absolute error $\epsilon_\mathrm{abs}=|\mathrm{cov}(X_1,X_2)-\mathrm{cov}_\mathrm{app}(\mu_1,\mu_2)|$, tends to 0 when θ tends to 0. As we show in Appendix B.4, the covariance is of the same magnitude as θ, and the absolute approximation-error is of order $O(\theta^2)$. It follows that $\epsilon=O(\theta)$, which means that the relative error vanishes as θ tends to 0 from above.

Appendix B.4. Covariance approximation

Throughout the derivation, we assume that all moments of the spatial distribution are bounded. We want to find an approximation of the covariance between species 1 and species 2. We are interested in a fast time scale (τ), such that the covariance is governed by movement processes alone. Therefore, the positive transition processes for the two species X_1 and X_2 are

$$\begin{aligned}
T_1^+(X_1,X_2)&=\langle X_1E_1(X_2)\rangle\\
T_2^+(X_1,X_2)&=\langle X_2E_2(X_1)\rangle,
\end{aligned} \tag{B.13}$$

and similarly the negative transition processes are

$$\begin{aligned}
T_1^-(X_1,X_2)&=X_1E_1(X_2)\\
T_2^-(X_1,X_2)&=X_2E_2(X_1).
\end{aligned} \tag{B.14}$$

By definition

$$\mathrm{cov}(X_1, X_2) = \langle (X_1 - \langle X_1 \rangle)(X_2 - \langle X_2 \rangle) \rangle \,, \tag{B.15}$$

and we can find an approximation of $\mathrm{cov}\,(X_\mathrm{n}, X_\mathrm{p})$ by applying eqs. (B.6,B.7) with $Q = 2$. We then find that

$$\begin{aligned}
\Lambda_{1,1} &= (X_1 - \langle X_1 \rangle)(X_2 - \langle X_2 \rangle) \\
G_1^- &= X_1 E_1\,(X_2) \left(\frac{X_1 - \langle X_1 \rangle - 1}{X_1 - \langle X_1 \rangle} - 1 \right) \\
G_1^+ &= \langle X_1 E_1\,(X_2) \rangle \left(\frac{X_1 - \langle X_1 \rangle + 1}{X_1 - \langle X_1 \rangle} - 1 \right) \\
G_2^- &= X_2 E_2\,(X_1) \left(\frac{X_2 - \langle X_2 \rangle - 1}{X_2 - \langle X_2 \rangle} - 1 \right) \\
G_2^+ &= \langle X_2 E_2\,(X_1) \rangle \left(\frac{X_2 - \langle X_2 \rangle + 1}{X_2 - \langle X_2 \rangle} - 1 \right).
\end{aligned} \tag{B.16}$$

Then from eq. (B.7) we have

$$\begin{aligned}
&\frac{\mathrm{d}}{\mathrm{d}\tau}\mathrm{cov}(X_1, X_2) = \\
&= \Big\langle (X_1 - \langle X_1 \rangle)(X_2 - \langle X_2 \rangle) \Big[X_1 E_1\,(X_2) \left(\frac{X_1 - \langle X_1 \rangle - 1}{X_1 - \langle X_1 \rangle} - 1 \right) \\
&\quad + \langle X_1 E_1\,(X_2) \rangle \left(\frac{X_1 - \langle X_1 \rangle + 1}{X_1 - \langle X_1 \rangle} - 1 \right) \\
&\quad + X_2 E_2\,(X_1) \left(\frac{X_2 - \langle X_2 \rangle - 1}{X_2 - \langle X_2 \rangle} - 1 \right) \\
&\quad + \langle X_2 E_2\,(X_1) \rangle \left(\frac{X_2 - \langle X_2 \rangle + 1}{X_2 - \langle X_2 \rangle} - 1 \right) \Big] \Big\rangle.
\end{aligned} \tag{B.17}$$

After some algebra we find that

$$\begin{aligned}
&\frac{\mathrm{d}}{\mathrm{d}\tau}\mathrm{cov}(X_1, X_2) = \\
&\langle X_1 \rangle \langle X_2 E_2\,(X_1) \rangle + \langle X_2 \rangle \langle X_1 E_1\,(X_2) \rangle \\
&- \langle X_1 X_2 E_2\,(X_1) \rangle - \langle X_1 X_2 E_1\,(X_2) \rangle \,.
\end{aligned} \tag{B.18}$$

The terms of the expectations of the functions in eq. (B.18) can be expressed in two-variable Taylor expansions around $\langle X_1 \rangle$ and $\langle X_2 \rangle$. Given that θ is sufficiently small, the Taylor series needs to be expanded only to second order. To simplify the notation, we define $\mu_1 = \langle X_1 \rangle$ and $\mu_2 = \langle X_2 \rangle$. The Taylor approximations of the expectations (to the second order) are thus

$$\begin{aligned}
\langle X_1 E_1\,(X_2) \rangle &= \mu_1 E_1\,(\mu_2) + E_1'\,(\mu_2)\,\mathrm{cov}(X_1, X_2) + O(\theta^2) \\
\langle X_2 E_2\,(X_1) \rangle &= \mu_2 E_2\,(\mu_1) + E_2'\,(\mu_1)\,\mathrm{cov}(X_1, X_2) + O(\theta^2),
\end{aligned} \tag{B.19}$$

and

$$\begin{aligned}
&\langle X_1 X_2 E_1\,(X_2) \rangle = E_1\,(\mu_2)\,[\mu_1 \mu_2 + \mathrm{cov}(X_1, X_2)] \\
&+ E_1'\,(\mu_2)\,[\mu_2 \mathrm{cov}(X_1, X_2) + \mu_1 \mathrm{var}(X_2) + 2\mathcal{M}_{2,1}] + O(\theta^2) \\
&\langle X_1 X_2 E_2\,(X_1) \rangle = E_2\,(\mu_1)\,[\mu_1 \mu_2 + \mathrm{cov}(X_1, X_2)] \\
&+ E_2'\,(\mu_1)\,[\mu_1 \mathrm{cov}(X_1, X_2) + \mu_2 \mathrm{var}(X_1) + 2\mathcal{M}_{1,2}] + O(\theta^2).
\end{aligned} \tag{B.20}$$

When we substitute eqs. (B.19,B.20) into eq. (B.18), several terms cancel and we end up with an approximation of the time evolution of the covariance

$$\begin{aligned}
&\frac{\mathrm{d}}{\mathrm{d}\tau}\mathrm{cov}(X_1, X_2) = -\mathrm{cov}(X_1, X_2)\,(E_1\,(\mu_2) + E_2\,(\mu_1)) \\
&- E_1'\,(\mu_2)\,[\mu_1 \mathrm{var}(X_2) + 2\mathcal{M}_{1,2}] \\
&- E_2'\,(\mu_1)\,[\mu_2 \mathrm{var}(X_1) + 2\mathcal{M}_{2,1}] + O(\theta^2),
\end{aligned} \tag{B.21}$$

which has the stationary solution

$$\begin{aligned}
&\mathrm{cov}^*(X_1, X_2) = \\
&- \frac{E_1'\,(\mu_2)\,[\mu_1 \mathrm{var}(X_2) + 2\mathcal{M}_{1,2}] + E_2'\,(\mu_1)\,[\mu_2 \mathrm{var}(X_1) + 2\mathcal{M}_{2,1}]}{E_1\,(\mu_2) + E_2\,(\mu_1)} \\
&+ O(\theta^2),
\end{aligned} \tag{B.22}$$

which shows that an approximation to this order includes the variances and two other second order moments

$$\begin{aligned}
\mathcal{M}_{2,1} &= \left\langle (X_1 - \mu_1)^2 (X_2 - \mu_2) \right\rangle \\
\mathcal{M}_{1,2} &= \left\langle (X_1 - \mu_1)(X_2 - \mu_2)^2 \right\rangle.
\end{aligned} \tag{B.23}$$

When the density dependencies are weak (θ is small), the variances are expected to be close to Poisson variances ($\mathrm{var}_1 = \mu_1 + O(\theta)$, $\mathrm{var}_2 = \mu_2 + O(\theta)$), and the other second order moments are expected to be small not exceeding $O(\theta)$. As we see, under such circumstances the covariance eq. (B.22) is of order $O(\theta)$. We must evaluate, however, if the absloute approximation-error ϵ_abs remains as a term of order $O(\theta^2)$.

Since the variances and the second order moments in eq. (B.22) are multiplied by first order derivatives of E that are of order $O(\theta)$, we only need to find approximations of these moments to order $O(\theta)$ for them to fall out as $O(\theta^2)$ terms in the covariance (eq B.22).

From eq. (B.7), we know that the time evolution of the variance of X_1 is

$$\begin{aligned}
&\frac{\mathrm{d}}{\mathrm{d}\tau}\mathrm{var}(X_1) = \\
&\left\langle (X_1 - \mu_1)^2 \left[X_1 E_1\,(X_2) \left(\frac{(X_1 - \mu_1 - 1)^2}{(X_1 - \mu_1)^2} - 1 \right) \right.\right. \\
&\left.\left. + \langle X_1 E_1\,(X_2) \rangle \left(\frac{(X_1 - \mu_1 + 1)^2}{(X_1 - \mu_1)^2} - 1 \right) \right] \right\rangle,
\end{aligned} \tag{B.24}$$

which after algebraic manipulation simplifies to

$$\frac{\mathrm{d}}{\mathrm{d}\tau}\mathrm{var}(X_1) = 2\left((\mu_1+1)\left\langle X_1 E_1\left(X_2\right)\right\rangle - \left\langle X_1^2 E_1\left(X_2\right)\right\rangle\right), \tag{B.25}$$

where

$$\begin{aligned}&\left\langle X_1^2 E_1\left(X_2\right)\right\rangle = \\ &E_1\left(\mu_2\right)\left[\mu_1^2 + \mathrm{var}(X_1)\right] + 2E_1'\left(\mu_2\right)\left[\mu_1 \mathrm{cov}(X_1, X_2) + \mathcal{M}_{2,1}\right] + O(\theta^2).\end{aligned} \tag{B.26}$$

Substitution back into eq. (B.24) yields

$$\begin{aligned}&\frac{\mathrm{d}}{\mathrm{d}\tau}\mathrm{var}(X_1) = 2E_1\left(\mu_2\right)\left(\mu_1 - \mathrm{var}(X_1)\right) \\ &+ 2E_1'\left(\mu_2\right)\left[\mathrm{cov}(X_1, X_2) - \mu_1 \mathrm{cov}(X_1, X_2) - 2\mathcal{M}_{2,1}\right] + O(\theta^2),\end{aligned} \tag{B.27}$$

which has the stationary solution

$$\begin{aligned}&\mathrm{var}^*(X_1) = \\ &\mu_1 + \frac{E_1'\left(\mu_2\right)\left[\mathrm{cov}(X_1, X_2)(1-\mu_1)\right]}{E_1\left(\mu_2\right)} - \frac{2E_1'\left(\mu_2\right)\mathcal{M}_{2,1}}{E_1\left(\mu_2\right)} + O(\theta^2),\end{aligned} \tag{B.28}$$

and because the transition processes for X_1 and X_2 are symmetric we also know that

$$\begin{aligned}&\mathrm{var}^*(X_2) = \\ &\mu_2 + \frac{E_2'\left(\mu_1\right)\left[\mathrm{cov}(X_1, X_2)(1-\mu_2)\right]}{E_2\left(\mu_1\right)} - \frac{2E_2'\left(\mu_1\right)\mathcal{M}_{1,2}}{E_2\left(\mu_1\right)} + O(\theta^2),\end{aligned} \tag{B.29}$$

which reveals that the second term in each of eq. (B.28) and eq. (B.29) is of order $O(\theta^2)$ because they include products of the first order derivatives of the movement function with the covariance. This allows us to rewrite the variances as

$$\begin{aligned}\mathrm{var}^*(X_1) &= \mu_1 - \frac{2E_1'\left(\mu_2\right)\mathcal{M}_{2,1}}{E_1\left(\mu_2\right)} + O(\theta^2) \\ \mathrm{var}^*(X_2) &= \mu_2 - \frac{2E_2'\left(\mu_1\right)\mathcal{M}_{1,2}}{E_2\left(\mu_1\right)} + O(\theta^2),\end{aligned} \tag{B.30}$$

whereby the orders of $\mathcal{M}_{2,1}$ and $\mathcal{M}_{1,2}$ remains to be evaluated.

From eq. (B.7), we know that the time evolution of $\mathcal{M}_{2,1}$ is

$$\begin{aligned}&\frac{\mathrm{d}}{\mathrm{d}\tau}\mathcal{M}_{2,1} = \\ &= \Bigg\langle (X_1-\mu_1)^2(X_2-\mu_2)\Bigg[X_1 E_1\left(X_2\right)\left(\frac{(X_1-\mu_1-1)^2}{(X_1-\mu_1)^2} - 1\right) \\ &\quad + \left\langle X_1 E_1\left(X_2\right)\right\rangle\left(\frac{(X_1-\mu_1+1)^2}{(X_1-\mu_1)^2} - 1\right) \\ &\quad + X_2 E_2\left(X_1\right)\left(\frac{X_2-\mu_2-1}{X_2-\mu_2} - 1\right) \\ &\quad + \left\langle X_2 E_2\left(X_1\right)\right\rangle\left(\frac{X_2-\mu_2+1}{X_2-\mu_2} - 1\right)\Bigg]\Bigg\rangle.\end{aligned} \tag{B.31}$$

which after some algebra simplifies to

$$\begin{aligned}&\frac{\mathrm{d}}{\mathrm{d}\tau}\mathcal{M}_{2,1} = \\ &\left\langle X_1 E_1\left(X_2\right)\right\rangle\left[2\mathrm{cov}(X_1, X_2) - \mu_2(2\mu_1+1\right] \\ &+ \left\langle X_1 X_2 E_1\left(X_2\right)\right\rangle\left[2\mu_1+1\right] + 2\mu_2\left\langle X_1^2 E_1\left(X_2\right)\right\rangle \\ &- 2\left\langle X_1^2 X_2 E_1\left(X_2\right)\right\rangle + \left\langle X_2 E_2\left(X_1\right)\right\rangle\left(\mathrm{var}(X_1) - \mu_1^2\right) \\ &+ 2\mu_1\left\langle X_1 X_2 E_2\left(X_1\right)\right\rangle - \left\langle X_1^2 X_2 E_2\left(X_1\right)\right\rangle,\end{aligned} \tag{B.32}$$

where

$$\begin{aligned}&\left\langle X_1^2 X_2 E_1\left(X_2\right)\right\rangle = \\ &E_1\left(\mu_2\right)\left[2\mathrm{cov}(X_1, X_2)\mu_1 + \mathrm{var}(X_1)\mu_2 + \mu_1^2\mu_2 + 2\mathrm{M}_{2,1}\right] \\ &+ E_1'\left(\mu_2\right)\left[\mathrm{var}(X_2)\mu_1^2 + 2\mathrm{cov}(X_1, X_2)\mu_1\mu_2\right. \\ &\left.+ 4\mu_1\mathcal{M}_{1,2} + 2\mu_2\mathcal{M}_{2,1} + \mathcal{M}_{2,2}\right] + O(\theta^2)\end{aligned} \tag{B.33}$$

and

$$\begin{aligned}&\left\langle X_1^2 X_2 E_2\left(X_1\right)\right\rangle = \\ &E_2\left(\mu_1\right)\left[2\mathrm{cov}(X_1, X_2)\mu_1 + \mathrm{var}(X_1)\mu_2 + \mu_1^2\mu_2 + 2\mathcal{M}_{2,1}\right] \\ &+ E_2'\left(\mu_1\right)\left[\mathrm{cov}(X_1, X_2)\mu_1^2 + \mathrm{var}(X_1)\mu_2(3-\mu_1) + \mu_1\mu_2\right. \\ &\left.+ 4\mu_1\mathcal{M}_{2,1} + \mu_2\mathcal{M}_{3,0} + \mathcal{M}_{3,1}\right] + O(\theta^2).\end{aligned} \tag{B.34}$$

The stationary solution of eq. (B.32) is thus

$$\mathcal{M}_{2,1}^* = \frac{\mathrm{cov}(X_1, X_2)E_1\left(\mu_2\right)}{4E_1\left(\mu_2\right) + E_2\left(\mu_1\right)} + O(\theta), \tag{B.35}$$

and, hence, due to symmetry

$$\mathcal{M}_{1,2}^* = \frac{\mathrm{cov}(X_1, X_2)E_2\left(\mu_1\right)}{4E_2\left(\mu_1\right) + E_1\left(\mu_2\right)} + O(\theta), \tag{B.36}$$

which tells us, since the covariance is of order $O(\theta)$, that

$$\begin{aligned}\mathcal{M}_{2,1}^* &= O(\theta) \\ \mathcal{M}_{1,2}^* &= O(\theta),\end{aligned} \tag{B.37}$$

and consequently also that

$$\begin{aligned}\mathrm{var}^*(X_1) &= \mu_1 + O(\theta^2)\\ \mathrm{var}^*(X_2) &= \mu_2 + O(\theta^2).\end{aligned} \tag{B.38}$$

By substitution of eq. (B.37) and eq. (B.38) into eq (B.22), we confirm finally that

$$\mathrm{cov}^*(X_1, X_2) = -\mu_1\mu_2\frac{E_1'(\mu_2) + E_2'(\mu_1)}{E_1(\mu_2) + E_2(\mu_1)} + O(\theta^2), \tag{B.39}$$

and, hence, that we have a covariance approximation

$$\mathrm{cov}_{\mathrm{app}}(\mu_1, \mu_2) = -\mu_1\mu_2\frac{E_1'(\mu_2) + E_2'(\mu_1)}{E_1(\mu_2) + E_2(\mu_1)}, \tag{B.40}$$

where the relative error $\epsilon = O(\theta)$. It follows then, via division by $\mu_1\mu_2$ that the approximation of the per capita covariance becomes

$$C = -\frac{E_1'(\mu_2) + E_2'(\mu_1)}{E_1(\mu_2) + E_2(\mu_1)}, \tag{B.41}$$

and is valid whenever $\mu_1\mu_2 \neq 0$.

We can identify a special case for when the relative error do not behave as analytically predicted. Under circumstances where the movement functions are such that $|E_1' + E_2'|$ declines towards zero faster than a linear function, the covariance is no longer of the same order as θ. For instance, if the term tends to zero super-linearily the relative error will not vanish at small θ. However, this is a degenerate case that is avoided theoretically by simply requiring that $(E_1'(\mu_2) + E_2'(\mu_1)) \sim \theta$ which is equivalent to, and the reason for, condition eq. B.11 in Appendix B.3. The degenerate properties of the case is perhaps best illustrated by an example. Assume that $E_1(\mu_2) = e^{\theta\mu_2}$ and $E_2(\mu_1) = e^{-\theta\mu_1}$. Then the numerator in eq. B.39 can then written as $-\theta(c_1e^{\theta\mu_2} - c_2e^{\theta\mu_1})$ which always tends to zero as analytically predicted except for when $c_1 = c_2$ which case must be assumed to be infinitely rare in nature.

Appendix C. Stability criteria

We shall perform a stability analysis of the spatial Lotka-Volterra dynamics

$$\begin{aligned}u &= \frac{\mathrm{d}N}{\mathrm{d}t} = rN - \alpha NP(1+C),\\ v &= \frac{\mathrm{d}P}{\mathrm{d}t} = \eta\alpha NP(1+C) - mP,\end{aligned} \tag{C.1}$$

where N is the prey population density, P is the predator population density, and C is the per capita covariance. The system is at equilibrium (N^*, P^*) when $u = v = 0$, and we hereafter assume that $N = N^*$ and $P = P^*$. We make use of eq. (11) and make the substitution $r = \alpha P(1+C)$ and $m = \alpha\eta N(1+C)$. Then, the Jacobian matrix is

$$\mathbf{J} = \begin{bmatrix}J_{11} & J_{12}\\ J_{21} & J_{22}\end{bmatrix} = \begin{bmatrix}-\alpha NPC_N & -\alpha N(1+C+PC_P)\\ \alpha\eta P(1+C+NC_N) & \alpha\eta NPC_P\end{bmatrix}, \tag{C.2}$$

where we use the notation $C_N = \frac{\partial C}{\partial N}$ and $C_P = \frac{\partial C}{\partial P}$. The system is stable if the inequalities

$$\begin{aligned}\mathrm{tr}(\mathbf{J}) &= J_{11} + J_{22} < 0\\ \det(\mathbf{J}) &= J_{11}J_{22} - J_{12}J_{21} > 0,\end{aligned} \tag{C.3}$$

are true, otherwise, the system is unstable.

Appendix C.1. Determinant of the Jacobian matrix

The determinant of the Jacobian (eq. C.2) is

$$\alpha^2\eta NP(1+C)(1+C+PC_P+NC_N) > 0 \tag{C.4}$$

and should be positive for stability. We are interested here only in the sign of $\det(\mathbf{J})$. The multiplicative factor $\alpha^2\eta NP(1+C)$ is always greater than zero and can therefore be canceled. The inequality then reduces to

$$1 + C + PC_P + NC_N > 0. \tag{C.5}$$

We may now distinguish the four terms in eq. (C.5) by their approximation order such that corresponding to eq. (C.5) we write

$$1 + O(\theta) + O(\theta^2) + O(\theta^2) > 0, \tag{C.6}$$

whereby we see that in the approximation limit $\det(\mathbf{J}) > 0$ since $C > -1$. Realistic global mean densities is bounded and should even be expected to be small considering the spatial scale.

Appendix C.2. Trace of the Jacobian matrix

The trace of the Jacobian (eq. C.2) is

$$\alpha NP(\eta C_P - C_N) < 0, \tag{C.7}$$

and should be negative for stability. Since αNP is always greater than zero, the system is stable if

$$\eta C_P < C_N. \tag{C.8}$$

By explicitly expressing C in terms of emigration-rate responses we find that eq. (C.8) is equivalent to

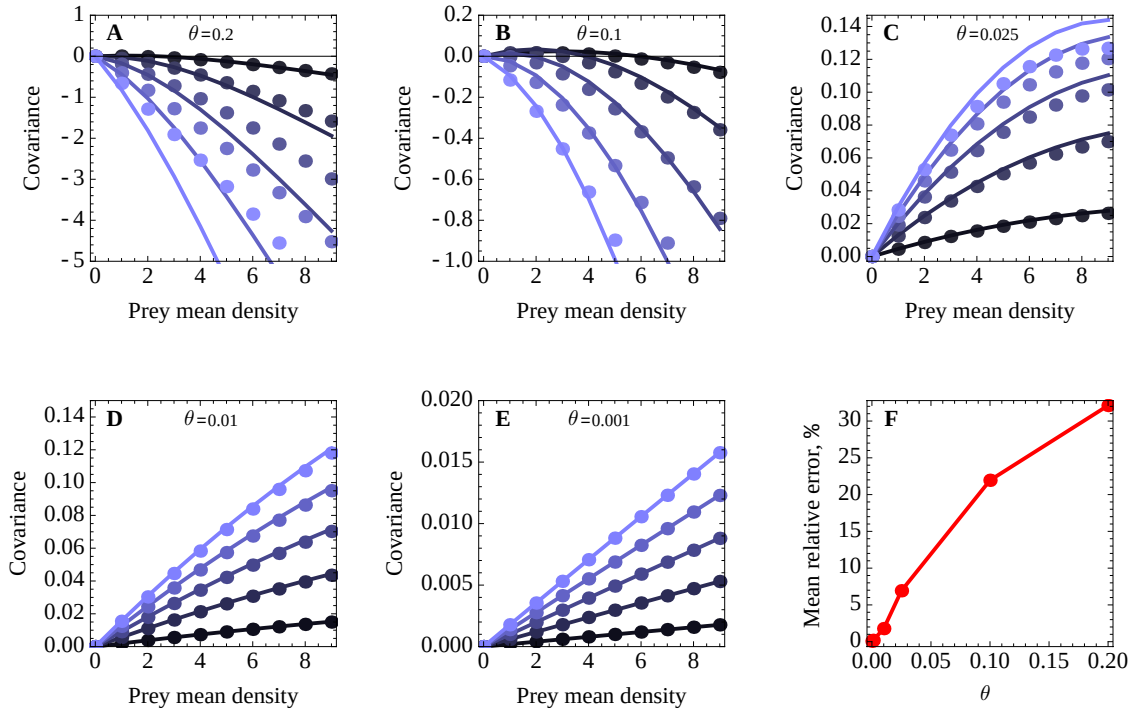

Figure C.7: **A-E** Covariance approximation $\mathrm{cov}_{\mathrm{app}}(N,P)$ (lines) compared to the exact covariance of a numerical solution of the master equation (dots) depending on values of the reactivity constant θ, where $E_{\mathrm{n}}(P) = 1 + e^{\theta P}$ and $E_{\mathrm{p}}(N) = 1 + 2e^{-\theta N}$. The different colors denote, from dark to bright, predator mean densities $\{1,3,5,7,9\}$. **F** Mean relative error (MRE) depending on θ.

$$E''_{\mathrm{p}} - \eta E''_{\mathrm{n}} - C\left(-E'_{\mathrm{p}} + \eta E'_{\mathrm{n}}\right) < 0, \tag{C.9}$$

and eq. (C.9) can also be expressed in the "categorical" form

$$Z'' - Z'C < 0, \tag{C.10}$$

where $Z'' = E''_{\mathrm{p}} - \eta E''_{\mathrm{n}}$ and $Z' = -E'_{\mathrm{p}} + \eta E'_{\mathrm{n}} > 0$.

Appendix C.3. Note on eq. (C.10)

The stability criterion has the peculiar property that C, which encapsulate all the spatial information that affects the population dynamics (eq. 9), appears only in one of the two terms in eq. (14). It is indeed correct to expect, that if $C = 0$ then the corresponding movements of individuals adds nothing to the classical Lotka-Volterra model. Such a case is straight forward as it directly implies that the steepness of the emigration-rate responses are zero and, hence, so is also Z''. In order to appreciate the stability criterion, which is used to be evaluated primarily in the limit where density-dependent movements have only weak effects on the population dynamics, it is important to recall that the emigration responses are the sum of the density independent movement component and the density-dependent movement component. If the density-dependent movement components are linear, then Z'' is necessarily zero. However, when any of the two species' density-dependent movement components are non-linear, their effects on the population dynamics can be weak by two different reasons: (i) when the density-dependent movement components flattens out and therefore tend to have only little dependence on densities, and (ii) when the density-dependent movement components are not altered but the independent movement component is in relation many times larger. In the first case Z'' approaches zero along with C, but in the second case Z'' is completely unaffected by the relatively large density independent movement component and the stabilizing properties of Z'' can therefore be studied.

Appendix D. Performance of the covariance approximation

Overall, the covariance approximation performs very well for small values of θ. The results we present here are for a case system in which the prey emigration-rate response was accelerating and the predator emigration-rate response was decelerating, which is a movement pattern that is commonly observed in empirical studies (see section 3.4). Figure C.7 provides graphical representations of the covariance (dotted) and the covariance approximation (Figure C.7 A-C), as well as the relative approximation-error (Figure C.7 D).

The mean relative error (MRE) of the covariance approximation $\mathrm{cov}_{\mathrm{app}}(N,P)$ was tested against the exact (apart from small numerical errors) covariance $\mathrm{cov}(X_{\mathrm{n}}, X_{\mathrm{p}})$, which was calculated from numerical equilibrium solutions of the master equa-

tion. For a set of values of θ, the mean relative error

$$\mathrm{MRE} = \frac{100}{N_{\max} P_{\max}} \sum_{N=0}^{N_{\max}} \sum_{P=0}^{P_{\max}} \left| 1 - \frac{\mathrm{cov}_{\mathrm{app}}(N,P)}{\mathrm{cov}(X_{\mathrm{n}}, X_{\mathrm{p}})_{\langle X_{\mathrm{n}} \rangle = N, \langle X_{\mathrm{p}} \rangle = P}} \right|, \tag{D.1}$$

was calculated. The MRE is a percentage measure of the average deviation of $\mathrm{cov}_{\mathrm{app}}(N,P)$ from $\mathrm{cov}(X_{\mathrm{n}}, X_{\mathrm{p}})_{\langle X_{\mathrm{n}} \rangle = N, \langle X_{\mathrm{p}} \rangle = P}$.

Some data points where excluded from the calculation of MRE:

1) Points where $\mathrm{cov}_{\mathrm{app}}(N,P) = 0$ will always give MRE = 100 as long as $\mathrm{cov}(X_{\mathrm{n}}, X_{\mathrm{p}})_{\langle X_{\mathrm{n}} \rangle = N, \langle X_{\mathrm{p}} \rangle = P}$ is not exactly zero. Numerical errors, albeit very small, in the equilibrium solution of the master equation make the case $\mathrm{cov}(X_{\mathrm{n}}, X_{\mathrm{p}})_{\langle X_{\mathrm{n}} \rangle = N, \langle X_{\mathrm{p}} \rangle = P} = 0$ rare. Therefore, points where $\mathrm{cov}_{\mathrm{app}}(N,P) = 0$ were excluded.

2) Points where the numerical covariance was less than one percent of the maxima of the (N,P) covariance surface, were excluded. This was because numerical errors affected the estimation of MRE at points where the covariance was very close to zero (relative to the maximum of the covariance surface).

References

Abrams, P.A., 2007. Habitat choice in predator-prey systems: Spatial instability due to interacting adaptive movements. American Naturalist 169, 581–594.

van Baalen, M., Sabelis, M.W., 1993. Coevolution of patch selection-strategies of predator and prey and the consequences for ecological stability. American Naturalist 142, 646–670.

van Baalen, M., Sabelis, M.W., 1999. Nonequilibrium population dynamics of "Ideal and free" prey and predators. American Naturalist 154, 69–88.

Bell, A., Rader, R., Peck, S., Sih, A., 2009. The positive effects of negative interactions: Can avoidance of competitors or predators increase resource sampling by prey? Theoretical Population Biology 76, 52–58.

Bernstein, C., 1984. Prey and predator emigration responses in the acarine system tetranychus urticae-phytoseiulus persimilis. Oecologia 61, 134–142.

Brown, J., 1988. Patch use as an indicator of habitat preference, predation risk, and competition. Behavioral Ecology and Sociobiology 22, 37–47.

Charnov, E.L., 1976. Optimal foraging, the marginal value theorem. Theoretical Population Biology 9, 129–136.

Cressman, R., Krivan, V., Garay, J., 2004. Ideal free distributions, evolutionary games, and population dynamics in multiple-species environments. American Naturalist 164, 473–489.

Dieckmann, U., Law, R., 2001. Relaxation projections and the method of moments, in: The Geometry of Ecological Interactions: Simplifying Spatial Complexity. Cambridge University Press, Cambridge, pp. 412–455.

Dieckmann, U., Law, R., Metz, J.A.J., 2001. The Geometry of Ecological Interactions. Cambridge University Press, Cambridge, UK.

Diehl, S., Cooper, S.D., Kratz, K.W., Nisbet, R.M., Roll, S.K., Wiseman, S.W., Jenkins, Jr., T.M., 2000. Effects of multiple, predator-induced behaviors on short-term producer-grazer dynamics in open systems. American Naturalist 156, 293–313.

Englund, G., Hambäck, P.A., 2004. Scale dependence of emigration rates. Ecology 85, 320–327.

Flaxman, S.M., Lou, Y., Meyer, F.G., 2011. Evolutionary ecology of movement by predators and prey. Theoretical Ecology 4, 255–267.

Forrester, G.E., 1994. Influences of predatory fish on the drift dispersal and local density of stream insects. Ecology 75, 1208–1218.

French, D.R., Travis, J.M.J., 2001. Density-dependent dispersal in host-parasitoid assemblages. Oikos 95, 125–135.

Gardiner, C., 2009. Stochastic Methods. Springer-Verlag, Berlin Heidenberg. fourth edition.

Godfray, H., Pacala, S., 1992. Aggregation and the population-dynamics of parasitoids and predators. American Naturalist 140, 30–40.

Hassell, M.P., 1971. Mutual interference between searching insect parasites. The Journal of Animal Ecology , 473–486.

Hauzy, C., Hulot, F.D., Gins, A., Loreau, M., 2007. Intra- and interspecific density-dependent dispersal in an aquatic prey-predator system. Journal of Animal Ecology 76, 552–558.

Iwasa, Y., 1982. Vertical migration of zooplankton: A game between predator and prey. The American Naturalist 120, 171.

Jenner, W.H., Roitberg, B.D., 2008. Foraging behaviour and patch exploitation by campoplex dubitator (Hymenoptera: ichneumonidae), a parasitoid of bark-mining larvae. Journal of Insect Behavior 22, 257–272.

van Kampen, N.G., 2007. Stochastic Processes in Physics and Chemistry. Elsevier, Amsterdam. third edition.

Keeling, M., Wilson, H., Pacala, S., 2002. Deterministic limits to stochastic spatial models of natural enemies. American Naturalist 159, 57–80.

Kratz, K.W., 1996. Effects of stoneflies on local prey populations: mechanisms of impact across prey density. Ecology 77, 1573–1585.

Krivan, V., 1997. Dynamic ideal free distribution: Effects of optimal patch choice on predator-prey dynamics. American Naturalist 149, 164–178.

Krivan, V., 1998. Effects of optimal antipredator behavior of prey on predator-prey dynamics: The role of refuges. Theoretical Population Biology 53, 131–142.

Krivan, V., Cressman, R., Schneider, C., 2008. The ideal free distribution: A review and synthesis of the game-theoretic perspective. Theoretical Population Biology 73, 403–425.

Maeda, T., Takabayashi, J., Yano, S., Takafuji, A., 1998. Factors affecting the resident time of the predatory mite phytoseiulus persimilis (Acari : Phytoseiidae) in a prey patch. Applied Entomology and Zoology 33, 573–576.

Mchich, R., Auger, P., Poggiale, J., 2007. Effect of predator density dependent dispersal of prey on stability of a predator-prey system. Mathematical Biosciences 206, 343–356.

Murdoch, W.W., Briggs, C.J., Nisbet, R.M., 2003. Consumer-Resource Dynamics. Princeton University Press, New Jersey.

Murdoch, W.W., Stewart-Oaten, A., 1989. Aggregation by parasitoids and predators: Effects on equilibrium and stability. American Naturalist 134, 288–310.

Nachappa, P., Margolies, D.C., Nechols, J.R., 2006. Resource-dependent giving-up time of the predatory mite, phytoseiulus persimilis. Journal of Insect Behavior 19, 741–752.

Ohara, Y., Takabayashi, J., 2012. Effects of larval densities and the duration since larval infestation on the host-searching behavior of diadegma semiclausum, a parasitoid of diamondback moth larvae on plants. Journal of Ethology 30, 295–300.

Rohani, P., Godfray, H.C.J., Hassell, M.P., 1994. Aggregation and the dynamics of host-parasitoid systems - a discrete-generation model with within-generation redistribution. American Naturalist 144, 491–509.

Roll, S.K., Diehl, S., Cooper, S.D., 2004. Effects of grazer immigration and nutrient enrichment on an open algae-grazer system. Oikos 108, 386–400.

Schreiber, S.J., Vejdani, M., 2006. Handling time promotes the coevolution of aggregation in predator-prey systems. Proceedings of the Royal Society B: Biological Sciences 273, 185–191.

Sih, A., 2005. Predator-prey space use as an emergent outcome of a behavioral response race, in: Ecology of Predator-prey Interactions. Oxford University Press, New York, pp. 240–255.

Zemek, R., Nachman, G., 1998. Interactions in a trirophic acarine predator-prey metapopulation system: effects of tetranychus urticae on the dispersal rates of phytoseiulus persimilis (Acarina: tetranychidae, phytoseiidae). Experimental and Applied Acarology 22, 259–278.